Crystal Structure and Magnetism of $(BEDT\text{-}TTF)_2MCl_4$ (BEDT-TTF = Bis(ethylenedithio)tetrathiafulvalene; M = Ga, Fe)

Mohamedally Kurmoo,*,†,‡ Peter Day,† Philippe Guionneau,§ George Bravic,§ Daniel Chasseau,§ Laurent Ducasse,|| Margaret L. Allan,⊥ Ian D. Marsden,⊥ and Richard H. Friend⊥

The Royal Institution of Great Britain, 21 Albemarle Street, London W1X 4BS, U.K., Laboratoire de Cristallographie et de Physique Cristalline, CNRS, ERS 133, Universite Bordeaux 1, 33405 Talence Cedex, France, Laboratoire de Physico-Chimie Theorique, CNRS, URA 503, Universite Bordeaux 1, 33405 Talence Cedex, France, and Cavendish Laboratory, University of Cambridge, Madingley Road, Cambridge CB3 0HE, U.K.

Received February 21, 1996[⊗]

The relation between crystal structure and bulk magnetic properties is investigated in the molecular charge transfer salts $(BEDT\text{-}TF)_2MCl_4$ (M = Ga, Fe). $(BEDT\text{-}TTF)_2GaCl_4$ crystallizes in the triclinic system. Its crystal structure consists of pairs of BEDT-TTF molecules arranged in layers with intermolecular S···S interactions. Band structure calculations predict semimetallic behavior contrary to the semiconductivity observed even under a pressure of 6 kbar (σ(300 K, 1 bar) = 10^{-1} S cm^{-1} and E_A = 0.2eV). The static (Faraday and SQUID magnetometry) and spin (EPR) susceptibilities indicate low-dimensional Heisenberg antiferromagnetic behavior with the susceptibility tending to zero as the temperature approaches zero. The data are analyzed using several low-dimensional magnetic models and are best fitted to a model consisting of two different spin dimers (Δ_1 = 108 K and Δ_2 = 212 K). The static magnetic susceptibility of $(BEDT\text{-}TTF)_2FeCl_4$ is modeled by a sum of Curie−Weiss ($S = {}^5/_2$ for Fe(d^5) and Θ = −4 K), χ_{tip}, and single dimer (Δ = 45 K) parameters. The BEDT-TTF layers in these compounds thus behave as Mott−Hubbard-localized systems, and the interaction between the magnetic moment on the Fe with those on the organic layer is negligible.

Introduction

The transition from localized to delocalized ground states in inorganic and organic molecular systems has long been a subject of controversy.[1] In particular, for organic conductors the competition between several ground states is more delicate since it can be controlled by very slight differences in the crystal structures.[2,3] Charge-transfer salts of the BEDT-TTF (BEDT-TTF = bis(ethylenedithio)tetrathiafulvalene) family, for example, embrace both localized and delocalized systems which display semiconducting, metallic, and superconducting electrical properties and Pauli paramagnetic, low-dimensional (1D and 2D) antiferromagnetic, and 3D-ordered (antiferromagnetic and weak ferromagnetic) ground states.[4] Such a range of behaviors arises from the variety of crystal packing and electronic band structures. Thus, one of the dilemmas facing chemists trying to synthesize organic conductors and superconductors is that they have exquisite control over the design of individual molecules but practically no control over designing molecular packing patterns in solid-state materials. We have been engaged in the past years in correlating the electrical and magnetic properties of BEDT-TTF charge-transfer salts with the crystal and electronic band structures with the aim of deriving synthetic guidelines.[5−10] Our present conclusion is that despite notable advances in extending the range of packing motifs by tuning the size, shape, and the charge of the anions, there are still no general synthetic tools available for controlling the crystal structures.

Isostructural compounds have been obtained by choosing similar anions (*e.g.*, I_3^-, IBr_2^-, AuI_2^-).[3] For example, several salts of the two superconducting phases (β and κ) have been synthesized and correlations between structures and supercon-

† The Royal Institute of Great Britain.

‡ Present address: Institut de Physique et Chimie des Materiaux de Strasbourg, 23 rue de Loess, F-67037 Strasbourg Cedex, France.

§ CRNS, ERS 1333.

|| CRNS, URA 503.

⊥ University of Cambridge.

⊗ Abstract published in *Advance ACS Abstracts,* July 1, 1996.

(1) (a) Mott, N. F. *Metal-Insulator Transitions*; 2nd ed.; Taylor Francis Publ.: London, 1990. (b) *Metal-Insulator Transition Revisited*; Edwards, P. P., Rao, C. N. R., Eds.; Taylor Francis Publ.: London, 1995.

(2) (a) Ishiguro, T; Yamaji, K. *Organic Superconductors*; Springer Verlag: Berlin, 1990. (b) *Organic Superconductivity*; Kresin, V. Z., Little, W., Eds.; Plenum: New York, 1990.

(3) Williams, J. M.; Ferraro, J. R.; Thorn, R. J.; Carlson, K. D.; Geiser, U.; Wang, H. H.; Kini, A. M.; Whangbo, M-H. *Organic Superconductors (including Fullerenes)*; Prentice Hall: Englewood Cliffs, NJ, 1992.

(4) See for example: Proceedings of the International Conference on Synthetic Metals. *Synth. Met.* **1987**, *19*; **1989**, *27*; **1991**, *42*; **1993**, *56*; **1995**, *71*.

(5) Day, P.; Kurmoo, M.; Mallah, T.; Marsden, I. R.; Friend, R. H.; Pratt, F. L.; Hayes, W.; Chasseau, D.; Gaultier, J.; Bravic, G.; Ducasse, L. *J. Am. Chem. Soc.* **1992**, *114*, 10722.

(6) Marsden, I. R.; Allan, M. L.; Friend, R. H.; Kurmoo, M.; Kanazawa, D.; Day, P.; Chasseau, D.; Bravic, G.; Ducasse, L. *Phys. Rev.* **1994**, *B50*, 2118.

(7) Kurmoo, M.; Day, P.; Stringer, A. M.; Howard, J. A. K.; Ducasse, L.; Pratt, F. L.; Singleton, J.; Hayes, W. *J. Mater. Chem.* **1993**, *3*, 1161.

(8) Rosseinsky, M. J.; Kurmoo, M.; Day, P.; Marsden, I. R.; Friend, R. H.; Chasseau, D.; Gaultier, J.; Bravic, G.; Ducasse, L. *J. Mater. Chem.* **1993**, *3*, 801.

(9) Bellitto, C.; Bonamico, M.; Fares, V.; Federici, F.; Righini, G.; Kurmoo, M.; Day, P. *Chem. Mater.* **1995**, *7*, 1475.

(10) Kurmoo, M.; Graham, A. W.; Day, P.; Coles, S. J.; Hursthouse, M. B.; Caulfield, J. L.; Singleton, J.; Pratt, F. L.; Hayes, W.; Ducasse, L.; Guionneau, P. *J. Am. Chem. Soc.* **1995**, *117*, 12209.

(11) (a) Yamochi, H.; Komatsu, T.; Matsukawa, N.; Saito, G.; Mori, T.; Kusunoki, M.; Sakaguchi, K. *J. Am. Chem. Soc.* **1993**, *115*, 11319. (b) Williams, J. M.; Schultz, A. J.; Wang, H. H.; Carlson, K. D.; Beno, M. A.; Emge, T. J.; Geiser, U.; Hawley, M. E.; Gray, K. E. *Physica* **1986**, *143B*, 346. (c) Saito, G.; Urayama, H.; Yamochi, H.; Oshima, K. *Synth. Met.* **1988**, *27*, A331.

S0020-1669(95)01456-X CCC: $12.00

ducting critical temperatures have been drawn.[11] Similar success was experienced for other phases with linear anions such as α and α′, which were found to have metal−semiconductor and semiconductor−semiconductor transitions, respectively. Similarly, it is possible to replace the donor BEDT-TTF in α-(BEDT-TTF)$_2$I$_3$ by BEDT-TSF and BEDT-STF (BEDT-TSF = bis(ethylenedithio)tetraselenafulvalene; BEDT-STF = bis(ethylenedithio)diselenadithiafulvalene).[12] We have employed such a strategy to study the interaction between localized moments on the anion and the electrons in the conduction band formed by the organic donor. Thus we have used $GaCl_4^-$ as the nonmagnetic counterpart to the magnetic $FeCl_4^-$. In both cases salts of a 2:1 stoichiometry with BEDT-TTF are obtained, which have similar structures and behave as semiconductors. Recently, Naito et al.[13] have used the same two anions to crystallize isostructural salts with BEDS-TTF (BEDS-TTF = bis(ethylenediselena)tetrathiafulvalene), where the $GaCl_4^-$ salt is a superconductor ($T_c \sim 8$ K) and the $FeCl_4^-$ salt shows a metal−insulator transition at *ca*. 8 K. However, the BEDT-TTF salts are not isostructural with the BEDS-TTF salts.

We have reported the structure and properties of (BEDT-TTF)$_2$FeCl$_4$ previously and have given a brief note on the electrical and magnetic properties of (BEDT-TTF)$_2$GaCl$_4$.[14,15] We describe here the full crystal structure determination and electronic band structure calculation, electrical properties at high pressure, and the magnetic properties of (BEDT-TTF)$_2$GaCl$_4$. We also re-examine the magnetic properties of (BEDT-TTF)$_2$FeCl$_4$ considering our present findings and correlate the results with the crystal structures.

Experimental Section

Synthesis. BEDT-TTF, prepared by the method of Larsen and Lenoir,[16] was recrystallized twice from chloroform before use. [(CH$_3$)$_4$N]GaCl$_4$ was obtained as colorless needles by reacting [(CH$_3$)$_4$NCl] and GaCl$_3$ in degassed absolute ethanol under an inert atmosphere of argon. The purity was checked by chemical analysis. The charge-transfer salt was obtained by electrocrystallization of BEDT-TTF (20 mg) in CH$_2$Cl$_2$ (50 mL) containing [(CH$_3$)$_4$N]GaCl$_4$ (200 mg). A three-compartment cell equipped with platinum wire (0.5 mm) electrodes was used, with a constant applied current of 1−2 μA for 2 weeks. The crystals of (BEDT-TTF)$_2$GaCl$_4$ were black shiny needles of maximum dimensions 4 × 0.2 × 0.1 mm^3.

X-ray Crystal Structure. After the screening of many twinned crystals under the microscope and by Weissenberg photographs, a single crystal of dimension 0.46 × 0.1 × 0.06 mm^3 was found to give sharp and single Bragg reflections and was thus selected for intensity data collection using a Nonius CAD-4 with graphite-monochromatized Cu Kα ($\lambda = 1.5418$ Å) radiation. The unit cell parameters (Table 1) were obtained from accurately measured angles of 20 intense reflections with $13 < 2\theta < 51°$. The space group was found unambigously to be $P\bar{1}$. Intensities of 11 720 reflections were measured at room temperature and reduced to give 10 844 independent ones. Three reflections were monitored hourly, and a maximum variation of intensity or position of 0.05% was observed. Data were corrected for Lorentz and polarization. An empirical absorption correction based on ψ scans was applied.

The crystal structure was solved by direct methods using the package SIR88.[17] The hydrogen atoms were placed in theoretical positions (C−H = 1 Å) and refined isotropically in the last cycle. The carbon, sulfur, gallium, and chlorine atoms were refined anisotropically. The atomic positions and isotropic or anisotropic thermal factors were obtained by the least-squares method to a final $R = 0.047$ and $R_w = 0.048$, using 3295 reflections with $I \geq 3\sigma(I)$ for 835 parameters. Difference Fourier maps at the end of the refinement give residual electron density of less than ±1 e/Å^2. The considerable number of parameters with so few reflections results in high standard deviations. Attempts to refine with more reflections by taking all those larger than $2\sigma(I)$ results in a poorer reliability factor (7%) and similar accuracy in bond lengths and angles.

Table 1. Crystallographic Data for (BEDT-TTF)$_2$GaCl$_4$

$C_{20}H_{16}S_{16}GaCl_4$	fw = 980.9
$a = 31.911(6)$ Å	space group = $P\bar{1}$ (No. 2)
$b = 16.580(4)$ Å	$T = 298$ K
$c = 6.645(2)$ Å	$\lambda = 1.5418$ Å
$\alpha = 98.15(2)°$	$\rho_{calcd} = 1.878$ g cm^{-3}
$\beta = 85.60(2)°$	$\mu = 127.23$ cm^{-1}
$\gamma = 90.55(2)°$	$R = 4.7\%$[a]
$V = 3470$ Å^3	$R_w = 4.8\%$[a]
$Z = 4$	

[a] $R = \sum||F_o| - |F_c||/\sum|F_o|$. $R_w = [\sum w||F_o| - |F_c||^2/\sum w|F_o|]^{1/2}$. $w = 1/[\sigma^2 + 0.005F^2]$.

Transfer Integrals and Band Structure Calculation. The transfer integrals, band structure, and Fermi surface of (BEDT-TTF)$_2$GaCl$_4$ have been calculated within the semi-empirical extended Hückel theory[18] using a double-ζ basis set and tight binding.[19] We have checked that the results presented here are very close to the ones obtained using a single-ζ basis set.

Electrical Transport. Conductivity measurements were limited to the long axis (crystallographic *c*-axis) of the needle crystals. Data were collected by the four-probe method using both ac and dc techniques. No apparent difference was noted. Pressure experiments were performed in a clamp cell with a 1:1 mixture of pentane−isopentane as the pressure-transmitting fluid.[20] The contacts were made with 25 μm gold wire onto pre-evaporated gold pads.

Electron Spin Resonance. Spectra were collected on several single crystals as a function of angle and temperature. Crystals were mounted on a cut flat face of Spectrosil quartz rods using a smear of silicone grease. The spectrometer was a Varian E9 with a cavity operating in a TE_{102} mode at 9 GHz and 100 kHz field modulation. Variable temperatures (4−300 K) were effected by use of a continuous-flow Oxford Instruments cryostat and an ITC-4 temperature controller.

Static Magnetic Susceptibility. Data were recorded on cooling and warming two independent batches of randomly oriented crystals (6.55 and 7.16 mg) as well as for different applied magnetic fields on a homemade Faraday balance employing a Cahn microbalance. A third batch was measured on a MPMS-7 SQUID magnetometer in fields ranging from 10 G to 2 T. The data were corrected for the core diamagnetism estimated from the sums of Pascal constants amounting to -4.85×10^{-4} emu/formula unit.

Results

Crystal Structure. (BEDT-TTF)$_2$GaCl$_4$ crystallizes in the triclinic system $P\bar{1}$ (Table 1). The crystal habit is needlelike, parallel to the crystallographic *c* axis. The labeling scheme adopted is shown in Figure 1. The atomic coordinates and selected bond lengths and angles are given in Tables 2 and 3. The asymmetric unit contains four crystallographically independent BEDT-TTF molecules and two $GaCl_4^-$ ions. With $Z = 2$ the unit cell (Figure 2) contains four formula units of (BEDT-TTF)$_2$GaCl$_4$.

The structure consists of stacks of nonplanar BEDT-TTF molecules along b separated by $GaCl_4^-$ anions in the a direction.

(12) Inokuchi, M.; Tajima, H.; Kobayashi, A.; Ohta, T.; Kuroda, H.; Kato, R.; Naito, T.; Kobayashi, H. *Bull. Chem. Soc. Jpn.* **1995**, *68*, 547.
(13) (a) Naito, T. Ph.D. Thesis, Toho University, Japan, 1994. (b) Kobayashi, H.; Udagawa, T.; Tomita, H.; Bun, K.; Naito, T.; Kobayashi, A. *Chem. Lett.* **1993**, 1559. (c) Kobayashi, A.; Udagawa, T.; Tomita, H.; Naito, T.; Kobayashi, H. *Chem. Lett.* **1993**, 2179.
(14) Mallah, T.; Hollis, C.; Bott, S.; Kurmoo, M.; Day, P.; Allan, M.; Friend, R. H. *J. Chem. Soc., Dalton Trans.* **1990**, 859.
(15) Kurmoo, M.; Allan, M. L.; Friend, R. H.; Chasseau, D.; Bravic, G.; Day, P. *Synth. Met.* **1991**, *41*, 2127.
(16) Larsen, J.; Lenoir, C. *Synthesis* **1988,** *2*, 134.
(17) Burla, M. C.; Camalli, M.; Cascarano, G.; Giacovazzo, C.; Polidori, G.; Spagna, R.; Viterbo, J. *J. Appl. Crystallogr.* **1989**, *22*, 389.
(18) (a) Ducasse, L.; Abderrabba, A.; Hoarau, J.; Pesquer, M.; Gallois, B.; Gaultier, J. *J. Phys. C, Solid State Phys.* **1986**, *19*, 3805. (b) Hoffmann, R. J. *J. Chem. Phys.* **1963**, *39*, 1397.
(19) Ducasse, L.; Fritsch, A. *Solid State Commun.* **1994**, *91*, 201.
(20) Guy, D. R. P.; Friend, R. H. *J. Phys E: Sci. Instrum.* **1986**, *19*, 430.

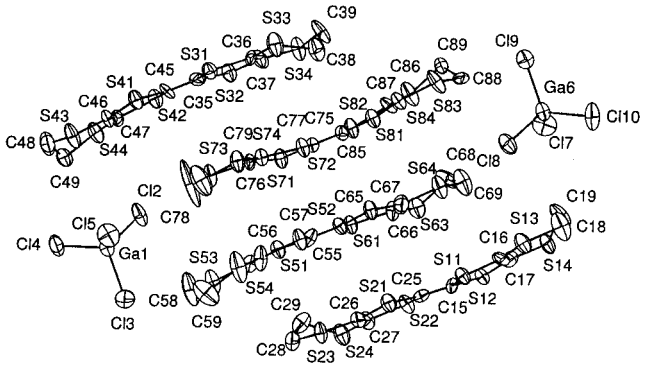

Figure 1. Labeling scheme adopted showing the thermal vibration ellipsoids.

The BEDT-TTF molecules in one stack form close S···S contacts with molecules in neighboring stacks along c to form layers. Molecules in each layer are parallel to one another.

The thermal parameters of the four independent BEDT-TTF molecules become progressively larger from the center of the molecules to the H_2C-CH_2 ends (Figure 1). The bond lengths and angles of the central TTF part of the molecules are thus more accurate than those in the outer parts. Some ethylene groups are disordered. The four crystallographically independent molecules belong to the same stack, and there are four different modes of overlap and average intermolecular distances between nearest neighbors (Figure 3). The average distance, calculated from the mean plane defined by the four inner sulfur atoms and the two central carbon atoms, between molecules I and IV is 3.35 Å, and the overlapping mode is bond-over-ring, which is quite favorable for large transfer integrals and thus high electrical conductivity. Between II and III, the distance is slightly longer, 3.41 Å, and the overlap is almost identical to the I/IV pair. The molecules in each dimer are parallel but translated along their long axes.

In contrast, the interplanar distances between I and II and between III and IV are much longer than the other two, 3.6 and 4.0 Å, respectively. The overlap between the latter pairs is also quite different; their long axes are twisted from one another by 34°. These irregular modes of overlap within the stacks lead to a strongly dimerized and alternate structure, with short intradimer and long interdimer separations. Each dimer is rotated with respect to its neighbors along the normal to the plane of the molecules. This structure resembles those reported for the $(BEDT\text{-}TTF)_2X$ set, where X is $FeCl_4^-$,[14] $InBr_4^-$, InI_4^-, and GaI_4^-.[21] The difference is that the latter compounds have only two independent molecules in the asymmetric unit and thus no alternation in interdimer distances. In the $GaCl_4^-$ salt one of the molecules in the stack is translated along its long axis so that there are some short atomic contacts between molecules from adjacent layers. These molecules then interrupt the regular spacing of the anions. Thus, there is a pair of anions in the cavities formed by the ethylenic hydrogen atoms. In the $FeCl_4^-$ and other MX_4^- salts there is no offset of the molecules in a layer, and we have a regular spatial distribution of anions with one anion per cavity.

The mode of overlap of the twisted molecules in $(BEDT\text{-}TTF)_2GaCl_4$ is the same as that observed in α′-$(BEDT\text{-}TTF)_2X$, X = $CuCl_2^-$, $Ag(CN)_2^-$, $Au(CN)_2^-$, and $AuBr_2^-$,[22−25] except that in this series all the molecules are twisted by 32° with respect to their neighbors. In $(BEDT\text{-}TTF)_2GaCl_4$ several short interstack S···S distances between equivalent molecules translated along *c* (3.40−3.52 Å) were observed to be less than the sum of van der Waals radii (S···S = 3.6 Å).

The C═C bond lengths range from 1.31 to 1.37 Å, from which one may assign charges between 0 and 0.5+ by comparison with neutral BEDT-TTF (1.32 Å) and $BEDT\text{-}TTF^{1/2+}$ (1.36 Å),[14,26] although the stoichiometry requires that the average charge per BEDT-TTF molecule be 0.5+. However it is possible that the lattice contains molecules of different charge but, because of the large number of structural parameters compared to the number of observable, the accuracy of the structure determination is too low to reach a conclusive judgement. Infrared reflectivity on a single crystal with the incident beam parallel and perpendicular to the needle axis shows in both cases a broad band centered at ∼1375 cm^{-1} with a width of ∼40 cm^{-1}. This band can be assigned to the C═C mode of the BEDT-TTF molecules. Since there are three such bonds per molecules and eight molecules per cell in addition to the low site symmetry of the molecules, it is very difficult to assign exact charge distribution among the independent molecules.

The $GaCl_4^-$ ions are almost tetrahedral with an average bond length of 2.164 Å. For each of the $GaCl_4^-$ anions, one of the Ga−Cl bond length (average 2.185 Å) is longer than the other three. The two independent $GaCl_4^-$ ions have similar environments but slightly different distances between the chlorine atoms and the thioethylene surrounding. Two short anion−cation distances (3.43 Å, Cl(20)···S(730); 3.481 Å, Cl(80)···S(640)) were observed between the sulfur atoms bonded to the disordered ethylene group (C−C distances of 1.31 and 1.40 Å).

Band Structure. The values of the intermolecular transfer integrals are indicated in Figure 4. The peculiar stacking of the BEDT-TTF molecules induces a strong alternation of the intrastack transfer integrals: the ratio of the intra- to interdimer integrals amounts to ∼6. The interstack integrals between the molecule I and its neighbors are very similar to the ones arising from molecule IV. On the other hand, the transfer integrals from molecule III are significantly larger than the ones from molecule II.

The corresponding band structure and Fermi surface are depicted in Figure 5. The highest occupied molecular orbital of the four independent molecules in the unit cell leads to four bands which are $^3/_4$ filled. The large gap between the two upper and the two lower bands is a direct consequence of the alternating intrastack transfer integrals. The existence of sizable interactions along *c*, roughly similar to the interdimer intrastack integrals, induces a dispersion along c*. As a consequence, the Fermi level cuts the two upper bands, so that the Fermi surface has both electron sheets and hole orbits which indicates semimetallic character. It is interesting that the band structure and Fermi surface are similar to those calculated for the superconductor $(BEDS\text{-}TTF)_2GaCl_4$ and yet it is a semiconductor.[27]

(21) (a) Beno, M. A.; Cox, D. D.; Williams, J. M.; Kwak, J. F. *Acta Crystallogr.* **1984**, *C40*, 1334. (b) Geiser, U.; Wang, H. H.; Schluter, J. A.; Hallenbeck, S. L.; Allen, T. J.; Chen, M. Y.; Kao, H. C. I.; Carlson, K. D.; Gerdom, L. E.; Williams, J. M. *Acta Crystallogr.* **1988**, *C44*, 1544.

(22) Kurmoo, M.; Talham, D. R.; Day, P.; Howard, J. A. K.; Stringer, A. M.; Obertelli, D. S.; Friend, R. H. *Synth. Met.* **1988**, *22*, 415.

(23) Guionneau, P.; Rahal, M.; Bravic, G.; Gaultier, J.; Mellado, J. M.; Chasseau, D.; Ducasse, L.; Kurmoo, M.; Day, P. *J. Mater. Chem.* **1995**, *5*, 1639.

(24) Beno, M. A.; Firestone, M. A.; Leung, P. C. W.; Sowa, L. M.; Wang, H. H.; Williams, J. M.; Whangbo M.-H. *Solid. State Commun.* **1986**, *57*, 735.

(25) Amberger, E.; Fuch, H.; Polborn, K. *Angew. Chem.* **1986**, *25*, 729.

(26) (a) Abboud, K. A.; Clevenger, M. B.; de Oliveira, G. F.; Talham, D. R. *J. Chem. Soc., Chem. Commun.* **1993**, 1560. (b) Chou, L-K.; Quijada, M. A.; Clevenger, M. B.; de Oliveira, G. F.; Abboud, K. A.; Tanner, D. B.; Talham, D. R. *Chem. Mater.* **1995**, *7*, 530.

(27) Montgomery, L. K.; Burgen, T.; Huffman, J. C.; Ren, J.; Whangbo, M.-H. *Physica* **1994**, *219C*, 490.

Table 2. Fractional Atomic Coordinates and B_{eq} Values (Å^2) for (BEDT-TTF)$_2$GaCl$_4$ at 298 K

	x/a	*y/b*	*z/c*	B_{eq}[a]		*x/a*	*y/b*	*z/c*	B_{eq}[a]
Ga(10)	0.01818(6)	0.2232(1)	0.6409(3)	3.6(1)	C(480)	0.0687(5)	−0.046(1)	0.709(3)	4.7(9)
Cl(20)	0.0763(1)	0.2379(3)	0.7907(7)	4.6(2)	C(490)	0.0693(5)	0.015(1)	0.891(3)	4.4(9)
Cl(30)	−0.0154(2)	0.3392(3)	0.6940(8)	4.7(2)	S(440)	0.1186(1)	0.0388(3)	0.9903(7)	3.8(2)
Cl(40)	−0.0210(1)	0.1342(3)	0.7707(8)	4.7(2)	C(470)	0.1499(4)	0.0438(9)	0.770(2)	2.4(6)
Cl(50)	0.0314(2)	0.1898(3)	0.3167(7)	5.3(2)	S(420)	0.1996(1)	0.0861(3)	0.8083(6)	3.1(2)
Ga(60)	0.50294(6)	0.7865(1)	0.2676(3)	3.8(1)	S(510)	0.1558(1)	0.5348(3)	0.5830(6)	3.1(2)
Cl(70)	0.4919(2)	0.8260(3)	0.5919(7)	5.3(2)	C(560)	0.1197(5)	0.4974(8)	0.408(2)	2.5(6)
Cl(80)	0.4436(1)	0.7654(3)	0.1331(7)	4.4(2)	S(530)	0.0724(1)	0.4635(3)	0.5070(7)	4.4(2)
Cl(90)	0.5378(1)	0.6710(3)	0.2198(8)	4.6(2)	C(580)	0.0477(6)	0.424(1)	0.279(3)	6.7(9)
Cl(100)	0.5384(2)	0.8767(3)	0.1265(8)	5.9(3)	C(590)	0.0567(6)	0.449(1)	0.090(3)	5.9(9)
S(110)	0.2805(1)	0.8985(3)	0.3093(6)	2.8(2)	S(540)	0.1071(2)	0.4610(4)	−0.0072(7)	6.3(3)
C(160)	0.3285(4)	0.9445(9)	0.355(2)	2.8(7)	C(570)	0.1336(5)	0.498(1)	0.212(2)	4.1(9)
S(130)	0.3613(1)	0.9494(3)	0.1353(7)	3.6(2)	S(520)	0.1833(1)	0.5368(3)	0.1533(6)	3.4(2)
C(180)	0.4082(6)	0.997(1)	0.232(3)	7.1(9)	C(550)	0.1930(5)	0.5649(8)	0.405(2)	2.2(6)
C(190)	0.4180(6)	0.988(1)	0.434(3)	5.4(9)	C(650)	0.2288(4)	0.6051(9)	0.464(2)	2.4(6)
S(140)	0.3806(1)	1.0205(3)	0.6418(7)	3.6(2)	S(610)	0.2387(1)	0.6351(3)	0.7153(6)	2.8(2)
C(170)	0.3355(5)	0.9715(8)	0.547(2)	2.7(6)	C(660)	0.2859(5)	0.6867(9)	0.660(2)	2.6(6)
S(120)	0.2958(1)	0.9565(3)	0.7358(6)	2.6(2)	S(630)	0.3080(1)	0.7361(3)	0.8776(7)	3.7(2)
C(150)	0.2625(4)	0.9065(8)	0.564(2)	1.9(6)	C(680)	0.3608(5)	0.742(1)	0.778(3)	5.3(9)
C(250)	0.2282(5)	0.8700(8)	0.626(2)	3.0(7)	C(690)	0.3696(6)	0.764(1)	0.585(3)	5.9(9)
S(210)	0.1954(1)	0.8143(3)	0.4502(6)	3.0(2)	S(640)	0.3465(1)	0.7185(3)	0.3642(7)	4.0(2)
C(260)	0.1550(4)	0.7938(9)	0.629(2)	2.6(7)	C(670)	0.2989(5)	0.6820(9)	0.470(3)	3.4(8)
S(230)	0.1122(1)	0.7404(3)	0.5301(7)	3.5(2)	S(620)	0.2691(1)	0.6269(3)	0.2866(6)	3.1(2)
C(280)	0.0815(5)	0.713(1)	0.756(3)	3.8(8)	S(710)	0.2451(1)	0.4009(3)	0.6672(6)	2.8(2)
C(290)	0.1056(6)	0.7099(9)	0.941(2)	3.4(8)	C(760)	0.2165(4)	0.3401(8)	0.479(2)	2.1(6)
S(240)	0.1274(1)	0.8074(3)	1.0371(7)	3.9(2)	S(730)	0.1717(1)	0.2954(3)	0.5840(7)	3.6(2)
C(270)	0.1612(5)	0.8213(9)	0.827(2)	3.1(7)	C(780)	0.1480(8)	0.260(2)	0.365(4)	13(2)
S(220)	0.2086(1)	0.8695(3)	0.8794(6)	2.7(2)	C(790)	0.1595(6)	0.266(1)	0.173(3)	6.6(9)
S(310)	0.2706(1)	0.1135(3)	0.2365(6)	2.7(2)	S(740)	0.2072(1)	0.2965(3)	0.0703(7)	3.6(2)
C(360)	0.3158(4)	0.1703(8)	0.284(2)	2.2(6)	C(770)	0.2308(4)	0.3443(8)	0.285(2)	2.8(7)
S(330)	0.3482(2)	0.1834(3)	0.0667(7)	4.4(2)	S(720)	0.2737(1)	0.4018(3)	0.2363(6)	2.8(2)
C(380)	0.3775(5)	0.271(1)	0.163(3)	4.5(9)	C(750)	0.2837(4)	0.4279(8)	0.494(2)	2.2(6)
C(390)	0.3976(4)	0.261(1)	0.357(3)	4.8(9)	C(850)	0.3195(4)	0.4661(8)	0.547(2)	2.2(6)
S(340)	0.3629(1)	0.2576(3)	0.5790(7)	4.1(2)	S(810)	0.3585(1)	0.4920(3)	0.3696(6)	2.8(2)
C(370)	0.3222(4)	0.199(1)	0.477(2)	3.5(7)	C(860)	0.3956(4)	0.5205(9)	0.551(2)	2.2(6)
S(320)	0.2840(1)	0.1731(3)	0.6616(6)	3.1(2)	S(830)	0.4437(1)	0.5527(3)	0.4423(7)	4.1(2)
C(350)	0.2526(4)	0.1172(9)	0.495(2)	2.8(7)	C(880)	0.4667(5)	0.6034(9)	0.669(3)	3.6(8)
C(450)	0.2166(4)	0.0832(9)	0.554(2)	2.2(6)	C(890)	0.4627(5)	0.5570(9)	0.845(3)	3.0(8)
S(410)	0.1827(1)	0.0299(3)	0.3862(6)	3.1(2)	S(840)	0.4108(1)	0.5497(3)	0.9563(7)	4.2(2)
C(460)	0.1418(4)	0.0168(9)	0.570(2)	2.7(6)	C(870)	0.3837(4)	0.5188(9)	0.745(2)	1.8(5)
S(430)	0.0966(1)	−0.0247(3)	0.4804(7)	4.5(2)	S(820)	0.3315(1)	0.4893(3)	0.8004(6)	3.1(2)

[a] $B_{eq} = {}^4/_3\sum_i\sum_j\beta_{ij}a_ia_j$.

Electrical Transport. Conductivity measurements on several crystals show semiconducting behavior with a room-temperature value of 10^{-1} S cm^{-1} (Figure 6) and an activation energy of 0.2 eV. Applying pressure increases the conductivity slightly while the activation energy remains constant up to 6 kbar. The room-temperature conductivity and activation energy are comparable to those of (BEDT-TTF)$_2$FeCl$_4$ and (BEDT-TTF)$_2$InBr$_4$ but quite different from (BEDT-TTF)$_2$GaI$_4$. The latter has surprisingly lower conductivity but a smaller activation energy.

Magnetism. The magnetic properties have been studied on a single crystal by EPR and on polycrystalline samples by Faraday and SQUID magnetometry. The EPR results will be presented first, followed by the static susceptibility results.

Electron Paramagnetic Resonance. At every temperature and crystal orientation the spectrum consists of a single Lorentzian signal, consistent with the low conductivity of the sample. The temperature dependence of the *g*-value and line width of the resonance line along three almost orthogonal axes is shown in Figures 7 and 8. Between 30 and 300 K the *g*-values are temperature independent and the line widths decrease smoothly. Below 30 K there is a gradual lowering of the *g*-value and a sharpening of the line width along two orientations but a broadening along the third axis. This is accompanied by an increase of the intensity of the resonance line along all three axes. The anomalies below 30 K may be due to small amount of paramagnetic impurities (see static susceptibility data below).

Static Susceptibility. At room temperature the susceptibility of (BEDT-TTF)$_2$GaCl$_4$ is 8×10^{-4} emu/formula unit. It increases to a broad maximum of 1.3×10^{-3} emu/formula unit at 80 K and shows a small Curie contribution at low temperatures (Figure 9). By removal of the latter (which is equivalent to ∼0.8% $S = {}^1/_2$ spins) the intrinsic susceptibility of the (BEDT-TTF)$_2$GaCl$_4$ crystals can be seen to tend to a value of zero emu/formula unit as the temperature approaches zero. The magnitude of the Curie tail is sample dependent; the bigger the crystals the smaller the Curie contribution, thus suggesting that it may originate from ends effects. For convenience, as will be shown later, the susceptibility is best discussed per unit cell as the content of the cell is eight molecules with a total of four spins, that is, two pairs of spin dimers ($S = {}^1/_2$).

Discussion

The anion GaCl$_4^-$ is diamagnetic with an effective volume between that of ClO$_4^-$ and InBr$_4^-$ and close to that of FeCl$_4^-$. Thus it should be an ideal diamagnetic diluent to replace the paramagnetic ($S = {}^5/_2$) FeCl$_4^-$ in (BEDT-TTF)$_2$FeCl$_4$ since it satisfies the requirements of size, shape, and charge. The structure of (BEDT-TTF)$_2$GaCl$_4$ contains dimers of BEDT-TTF which give rise to alternating weak and strong interdimer and intradimer transfer integrals along the stacks of face to face cations. Nevertheless, the band structure calculated within the extended Hückel formalism from the observed crystal structure predicts a semimetallic rather than the observed semiconducting

Table 3. Selected Bond Lengths (Å) and Angles (deg)

		$GaCl_4^-$	
Ga(10)−Cl(20)	2.167(5)	Ga(60)−Cl(70)	2.164(6)
Ga(10)−Cl(30)	2.182(6)	Ga(60)−Cl(80)	2.160(5)
Ga(10)−Cl(40)	2.155(5)	Ga(60)−Cl(90)	2.195(6)
Ga(10)−Cl(50)	2.157(6)	Ga(60)−Cl(100)	2.144(6)
Cl(20)−Ga(10)−Cl(30)	108.7(2)	Cl(70)−Ga(60)−Cl(80)	109.7(2)
Cl(20)−Ga(10)−Cl(40)	109.8(2)	Cl(70)−Ga(60)−Cl(90)	108.9(2)
Cl(20)−Ga(10)−Cl(50)	110.1(2)	Cl(70)−Ga(60)−Cl(100)	110.2(2)
Cl(30)−Ga(10)−Cl(40)	108.0(2)	Cl(80)−Ga(60)−Cl(90)	108.1(2)
Cl(30)−Ga(10)−Cl(50)	108.4(2)	Cl(80)−Ga(60)−Cl(100)	110.1(2)
Cl(40)−Ga(10)−Cl(50)	111.7(2)	Cl(90)−Ga(60)−Cl(100)	109.8(2)
		BEDT−TTF I	
C(150)−C(250)	1.31(2)		
C(150)−S(110)	1.73(2)	C(250)−S(210)	1.78(2)
S(110)−C(160)	1.73(2)	S(210)−C(260)	1.75(2)
C(160)−C(170)	1.33(2)	C(260)−C(270)	1.36(2)
C(170)−S(120)	1.75(2)	C(270)−S(220)	1.74(2)
S(120)−C(150)	1.74(2)	S(220)−C(250)	1.75(2)
S(120)−C(150)−S(110)	115.6(8)	S(220)−C(250)−S(210)	112.0(9)
C(150)−S(110)−C(160)	95.1(7)	C(250)−S(210)−C(260)	97.0(7)
S(110)−C(160)−C(170)	117(1)	S(210)−C(260)−C(270)	116(1)
C(160)−C(170)−S(120)	118(1)	C(260)−C(270)−S(220)	118(1)
C(170)−S(120)−C(150)	94.2(7)	C(270)−S(220)−C(250)	97.0(8)
		BEDT−TTF II	
C(350)−C(450)	1.33(2)		
C(350)−S(310)	1.76(2)	C(450)−S(410)	1.76(1)
S(310)−C(360)	1.74(2)	S(410)−C(460)	1.75(2)
C(360)−C(370)	1.33(2)	C(460)−C(470)	1.38(2)
C(370)−S(320)	1.76(2)	C(470)−S(420)	1.75(2)
S(320)−C(350)	1.72(2)	S(420)−C(450)	1.73(2)
S(320)−C(350)−S(310)	114.1(9)	S(420)−C(450)−S(410)	113.7(8)
C(350)−S(310)−C(360)	95.2(7)	C(450)−S(410)−C(460)	96.7(7)
S(310)−C(360)−C(370)	118(1)	S(410)−C(460)−C(470)	116(1)
C(360)−C(370)−S(320)	116(1)	C(460)−C(470)−S(420)	116(1)
C(370)−S(320)−C(350)	96.7(8)	C(470)−S(420)−C(450)	97.0(7)
		BEDT−TTF III	
C(550)−C(650)	1.37(2)		
C(550)−S(510)	1.73(2)	C(650)−S(610)	1.73(2)
S(510)−C(560)	1.75(2)	S(610)−C(660)	1.76(2)
C(560)−C(570)	1.34(2)	C(660)−C(670)	1.29(2)
C(570)−S(520)	1.74(2)	C(670)−S(620)	1.74(2)
S(520)−C(550)	1.72(2)	S(620)−C(650)	1.75(2)
S(520)−C(550)−S(510)	115.9(9)	S(620)−C(650)−S(610)	114.6(8)
C(550)−S(510)−C(560)	95.9(7)	C(650)−S(610)−C(660)	95.4(7)
S(510)−C(560)−C(570)	114(1)	S(610)−C(660)−C(670)	116(1)
C(560)−C(570)−S(520)	120(1)	C(660)−C(670)−S(620)	119(1)
C(570)−S(520)−C(550)	93.8(8)	C(670)−S(620)−C(650)	94.2(8)
		BEDT−TTF IV	
C(750)−C(850)	1.35(2)		
C(750)−S(710)	1.72(2)	C(850)−S(810)	1.74(2)
S(710)−C(760)	1.79(2)	S(810)−C(860)	1.77(2)
C(760)−C(770)	1.35(2)	C(860)−C(870)	1.32(2)
C(770)−S(720)	1.70(2)	C(870)−S(820)	1.72(2)
S(720)−C(750)	1.76(2)	S(820)−C(850)	1.74(2)
S(720)−C(750)−S(710)	115.3(9)	S(820)−C(850)−S(810)	114.5(8)
C(750)−S(710)−C(760)	94.5(7)	C(850)−S(810)−C(860)	94.8(7)
S(710)−C(760)−C(770)	115(1)	S(810)−C(860)−C(870)	118(1)
C(760)−C(770)−S(720)	120(1)	C(860)−C(870)−S(820)	116(1)
C(770)−S(720)−C(750)	94.7(7)	C(870)−S(820)−C(850)	95.7(7)

behavior. Evidently the localized electron behavior of $(BEDT\text{-}TTF)_2GaCl_4$ cannot be accounted for by the one-electron approach which supposes that the insulating character is mainly driven by symmetry considerations and band filling. Thus, semiconducting character is predicted for $^3/_4$ filled bands and

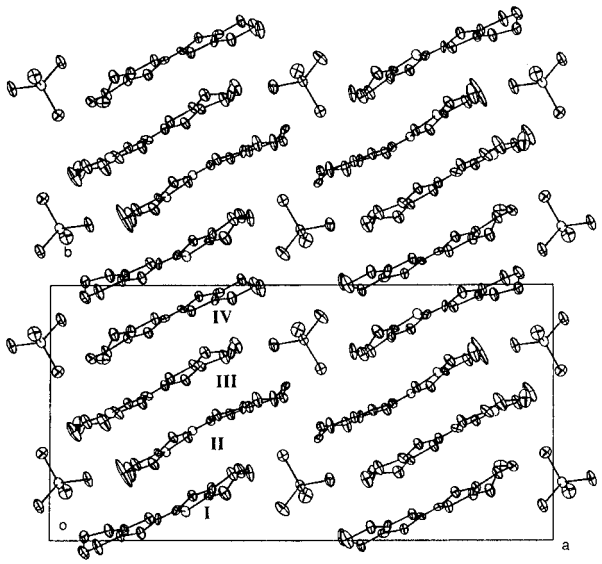

Figure 2. View of the unit cell along *c* showing the distortion of the molecules from planarity and the disorder of the ethylene groups.

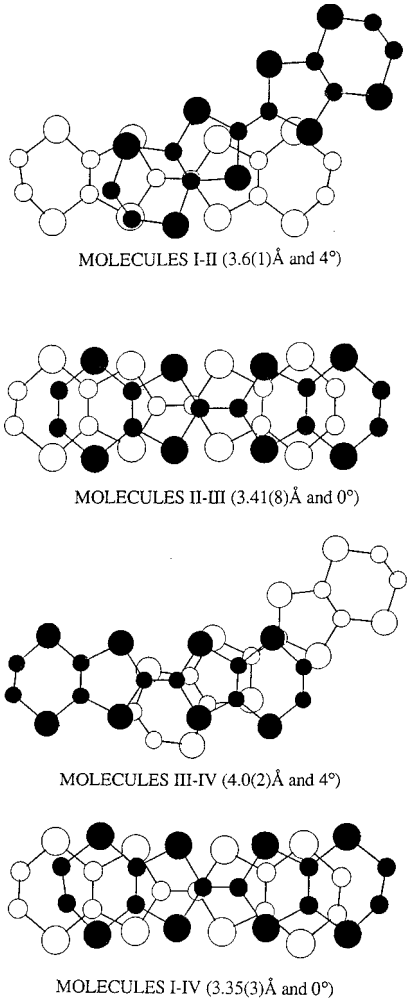

Figure 3. Modes of overlap between nearest-neighbor molecules.

is indeed found in $(MDT\text{-}TTF)_4Pt(CN)_4{\cdot}2H_2O$,[28] whose unit cell likewise contains 4 molecules with an average charge of $^1/_2+$. In this case the observed semiconducting state comes from a combination of a large ratio (∼3) of the two intradimer transfer integrals, together with small transverse interactions which results in small band dispersions. However, there are other cases of BEDT-TTF salts where semiconducting behavior is found either at room temperature or at low temperature (*e.g.*, BEDT-

(28) Mousdis, G. A.; Ducasse, L.; Fettouhi, M.; Ouahab, L.; Dupart, E.; Garrigou-Lagrange, C.; Amiell, J.; Canet, R.; Delhaes, P. *Synth. Met.* **1992**, *48*, 219.

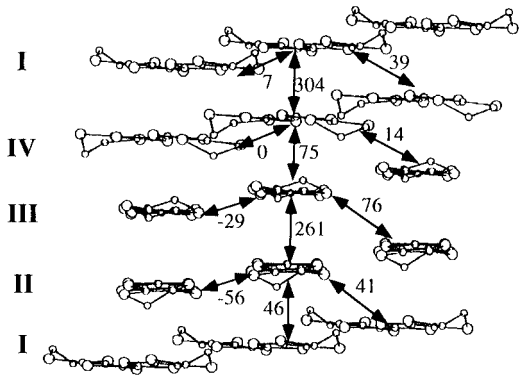

Figure 4. View of the layer along the central C═C bond of molecule II, showing the transfer integrals (meV) between neighboring molecules.

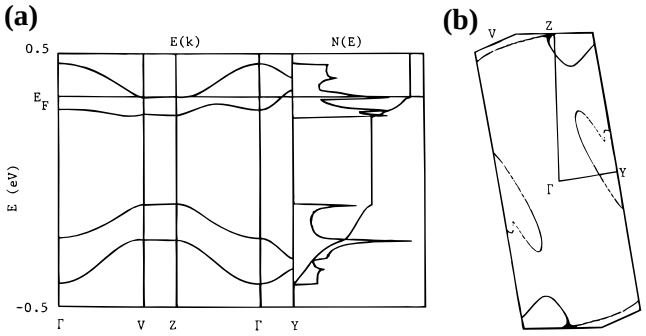

Figure 5. Band structure: (a) Energy dispersion and density of states; (b) Fermi surface.

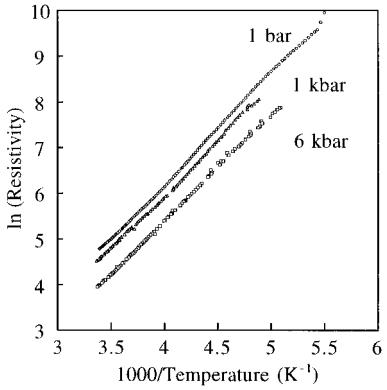

Figure 6. Temperature dependence of the electrical resistivity along *c* for three different applied pressures.

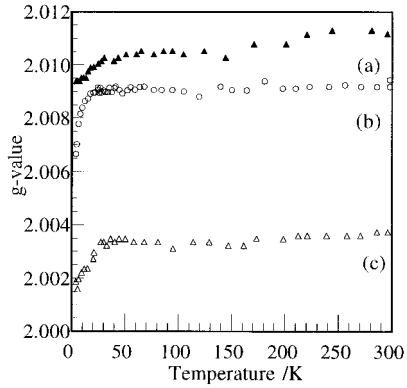

Figure 7. Temperature dependence of the *g*-values of the EPR signal along three orthogonal axes: (a, b) $H_o \perp c$; (c) $H_o \parallel c$.

$TTF)_4Cl_2 \cdot 6H_2O$[8]) even though the band structure predicts a metallic or semimetallic character. In that case an alternative must be sought to explain the localized ground state. One such is a multi-electron valence bond approach to analyze the effect

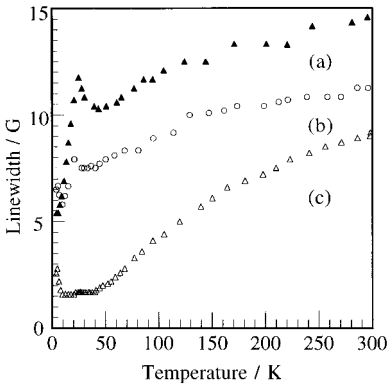

Figure 8. Temperature dependence of the peak-to-peak line widths of the EPR signal along three orthogonal axes: (a, b) $H_o \perp c$; (c) $H_o \parallel c$.

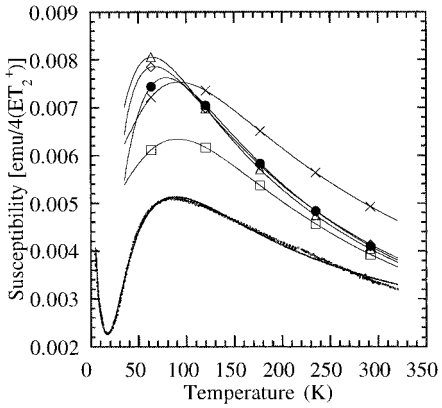

Figure 9. Temperature dependence of the magnetic susceptibility of $(BEDT\text{-}TTF)_2GaCl_4$ (open circles) and the theoretical model, Bonner−Fisher ($J/k_B = 70$ K, open squares), 2D-quadratic layer antiferromagnet ($J/k_B = 50$ K, open triangles), alternate chain ($\alpha = 0.7$, $J/k_B = 70$ K, open diamonds), spin ladder (closed circles), $S = 1$ Haldane chain ($J/k_B = 70$ K, crosses), and two-dimer fits (solid line).

of the electronic correlations.[29] According to that model, a correlation-driven localization may occur in $^3/_4$-filled 1D band systems, where there is strong dimerization along the molecular stacks. A correlation-driven localization may occur in systems where a stack dimerization is rather large. Some examples will illustrate the point.

In the α′ series of BEDT-TTF salts, which are localized at room temperature (*e.g.*, $(BEDT\text{-}TTF)_2AuBr_2$[30]) the ratio between the intra- and interdimer integral is about 3. Similarly, a ratio of 1.5 is found in $(BEDT\text{-}TTF)_4Cl_2 \cdot 6H_2O$,[8] which qualitatively explains the broad metal−semiconductor transition at low temperature, while in the $(BEDT\text{-}TTF)_4M(CN)_4$ (M = Ni, Pt) salts[31] the corresponding ratio is reduced to 1.29, which again could explain the existence of a metallic phase at high temperature and the transition to a semiconductor at 150 K. Finally, in the $(TMTTF)_2X$ series, the ratio is less than 1.5, again in agreement with the broad transition observed around 100−200 K.

The second and third of the examples just quoted share a common structural characteristic. Along the main stacking direction (perpendicular to the molecular plane), two modes of packing are found: one involves parallel BEDT-TTF molecules, while the second one invokes a twist angle of 34°. Just the same motif is found in $(BEDT\text{-}TTF)_2GaCl_4$, where in this case

(29) Fritsch, A.; Ducasse, L. *J. Phys. (Fr.)* **1991**, *1*, 855.
(30) Chasseau, D.; Gaultier, J.; Bravic, G.; Ducasse, L.; Kurmoo, M.; Day, P. *Proc. R. Soc. London A* **1993**, *442*, 207.
(31) Ducasse, L.; Mousdis, G. A.; Fettouhi, M.; Ouahab, L.; Amiell, J.; Delhaes, P. *Synth. Met.* **1993**, *56*, 1995.

the ratio of the intrastack integrals is 6. In comparison with the other examples, such a large ratio would be expected to lead to a localized regime already at room temperature.

The susceptibility of (BEDT-TTF)$_2$GaCl$_4$ is much higher than would be expected for a metallic system; the broad maximum indicates low-dimensional antiferromagnetic exchange while the fact that the susceptibility tends to zero at $T = 0$ K suggests a system with a magnetic gap. As already pointed out by several authors,[3,32] it is probable that Coulomb repulsion is large and the spins are localized with one spin for each BEDT-TTF dimer, consistent with the semiconducting nature of the salt. Similar behavior is found in α′-(BEDT-TTF)$_2$X, X = $CuCl_2$, $AuBr_2$, and $Ag(CN)_2$.[32] These salts are Mott−Hubbard insulators with poor π delocalization and large Coulomb repulsion between the conduction electrons. Their susceptibilities follow that of a 1-D $S = {}^1/_2$ antiferromagnet with $J/k_B \sim 55$ K. In addition, the $Ag(CN)_2$ and $AuBr_2$ salts undergo a spin-Peierls transition below 7 K, emphasizing the 1-D nature of these salts.[33]

The susceptibility of (BEDT-TTF)$_2$GaCl$_4$ is compared to the models for 1-D and 2-D antiferromagnets in Figure 9.[34,35] The curves have been calibrated for 4 mol of $S = {}^1/_2$ spins using the average experimental value of g (2.0078), and the value of the exchange interaction J/k_B (70 K for the 1D- and 50 K for the 2D-model) has been chosen to match the maximum in the measured susceptibility. It can be seen that the measured susceptibility at the maximum is only 70% to 80% of that predicted by the theoretical models and, furthermore, that both models have finite susceptibilities at $T = 0$ K and thus not appropriate to describe the magnetic properties of (BEDT-TTF)$_2$GaCl$_4$. To model the observed behavior more closely, various models were examined which predict a magnetic gap [Haldane ($S = 1$),[36] alternate chain,[37] singlet−triplet,[38] and spin ladder ($S = {}^1/_2$)[39]]. A better agreement between observed and calculated was obtained when we fitted the data to the following:

$$\chi_{obs} = n_s\chi_{model} + \chi_o + \chi_{Curie}$$

where n_s is the number of spins per unit cell and χ_o allows for any discrepancy from the estimated diamagnetic corrections and the temperature-independent paramagnetism that may arise from the system which contains low-lying excited states. The last term is the Curie contribution due to impurities and end effects.

To justify a Haldane system, one must first have a one-dimensional $S = 1$ chain. Since the molecules can have different charge, we consider the structure is made up of pairs of molecules carrying charge +1 each separated by chains of neutral dimers. Thus a $S = 1$ ground state requires that the triplet state be the most stable. Compounds containing (BEDT-TTF)$_2^{2+}$ units are invariably diamagnetic; thus, the singlet state is more stable. For example, (BEDT-TTF)$FeBr_4$,[14] (BEDT-TTF)$_4$[KFe(C$_2$O$_4$)$_3$]·C$_6$H$_5$CN,[40] and (BEDT-TTF)$_3$CuBr$_4$[41] contain dimers of BEDT-TTF$^+$ and all show no contribution to the susceptibility at low temperature. Nevertheless, the susceptibility of (BEDT-TTF)$_2$GaCl$_4$ does not fit the model of the Haldane chain and the magnitude of n_s is less than the number of spins in the unit cell. Figure 9 shows the theoretical curve for fixed $J/k_B = 70$ K, $n_s = 4$, and $\chi_o = \chi_{Curie} = 0$ in the temperature range 50 K ($T \geq J/2k_B$) to 320 K. Similar goodness of fit and n_s values were obtained for the alternate chain ($\alpha = 0.7-0.9$) and the spin ladder models. However, an acceptable value of n_s was obtained with a singlet−triplet model. The goodness of fit was improved when a model allowing for two gaps was employed, *i.e.*, two different spin dimers (Figure 9). The values of n_s and χ_o are 1.92 × 2 and 0.0013 emu/unit cell (or 0.0003 emu/formula unit), respectively. The two singlet−triplet energy separations are 108 K (9.3 meV) and 212 K (18.3 meV).

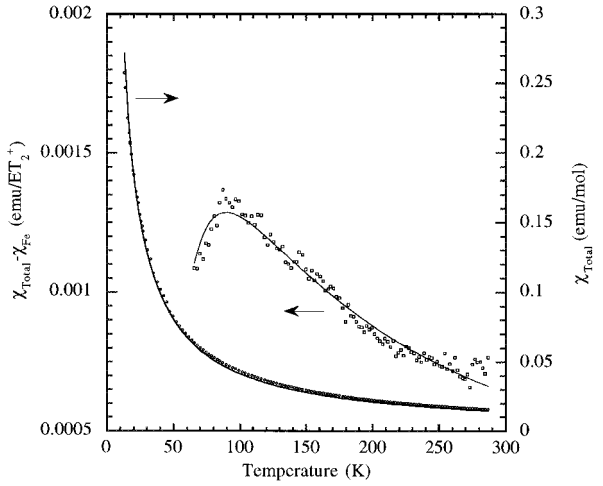

Figure 10. Temperature dependence of the observed magnetic susceptibility of (BEDT-TTF)$_2$FeCl$_4$ (open circles) and that of the BEDT-TTF contribution. The solid lines are the theoretical fits (see text).

In considering this conclusion about the ground state in (BEDT-TTF)$_2$GaCl$_4$, we have re-examined our earlier susceptibility data for (BEDT-TTF)$_2$FeCl$_4$. Previously we had interpreted the magnetic susceptibility as the sum of a Curie−Weiss term ($S = {}^5/_2$ and $\Theta = -5$ K) and a temperature-independent term. Here we have fitted the low-temperature data and extracted a value of the Weiss constant for fixed values of $S = {}^5/_2$ and $g = 2$ and then used the parameters ($S = {}^5/_2$, $g = 2$, $\Theta = -4$ K) of the fit to calculate the difference between observed and calculated at all temperatures to obtain the contribution from the BEDT-TTF. The resulting difference was fitted to a singlet−triplet model. The simplest model of a dimer ($\Delta = 45$ K and $n_s = 1$) gives the best fit to the data between 50 and 300 K. Figure 10 shows the observed data and the fit to

$$\chi_{obs} = n_s\chi_{dimer} + \chi_o + \chi_{Curie-Weiss}$$

together with the susceptibility minus the contribution from the anion and the fit to the dimer model and a temperature-independent term.

The number of spins per formula unit for an expected localized system emphasizes the importance of Coulomb repulsion and low-dimensional spin correlation in this com-

(32) (a) Obertelli, S. D.; Friend, R. H.; Talham, D. R.; Kurmoo, M.; Day, P. *J. Phys.: Condens. Matter* **1989**, *1*, 5671. (b) Parker, I. D.; Friend, R. H.; Kurmoo, M.; Day, P. *J. Phys.: Condens. Matter* **1989**, *1*, 5681.
(33) Kurmoo, M.; Green, M. A.; Day, P.; Bellitto, C.; Staulo, G. *Synth. Met.* **1993**, *55*−57, 2380 and unpublished results.
(34) (a) Bonner, J. C.; Fisher, M. E. *Phys Rev.* **1964**, *A135*, 640. (b) Hall, J. W.; Marsh, W. E.; Weller, R. R.; Hatfield, W. E. *Inorg. Chem.* **1981**, *20*, 1033.
(35) Lines, M. E. *J. Phys. Chem. Solids* **1970**, *31*, 101.
(36) (a) Meyers, A.; Gleizes, A.; Girerd, J. J.; Verdaguer, M.; Kahn, O. *Inorg. Chem.* **1982**, *21*, 1729. (b) Sandvik, A. W.; Kurkijärvi, J. *Phys. Rev. B* **1991**, *43*, 5950.
(37) Hatfield, W. E.; Estes, W. E.; Marsh, W. E.; Pickens, M. W.; ter Haar, L. W.; Weller, R. R. In *Linear Chain Compounds*; Miller, J. S., Ed.; Plenum Press: New York, 1983; Vol. 3, p 43.
(38) Bleaney, B.; Bowers, K. D. *Proc. R. Soc. London* **1952**, *A214*, 451.
(39) (a) Johnston, D. C.; Johnson, J. W.; Goshorn, D. P.; Jacobson, A. J. *Phys. Rev.* **1987**, *B35*, 219. (b) Barnes, T.; Riera, J. *Phys. Rev.* **1994**, *B50*, 6817.
(40) Day, P.; Graham, A. W.; Kepert; C. J.; Kurmoo, M. *Synth. Met.* **1995**, *70*, 767.
(41) (a) Guionneau, P.; Bravic, G.; Gaultier, J.; Chasseau, D.; Kurmoo; M.; Day, P. *Acta Crystallogr.* **1994**, *C50*, 1894. (b) Hebrard, S.; Bravic, G.; Gaultier, J.; Chasseau, D.; Kurmoo, M.; Day, P. *Acta Crystallogr.* **1994**, *C50*, 1892.

pound. Low-dimensional charge-transfer salts such as (BEDT-TTF)$_2$GaCl$_4$ are expected to behave as Heisenberg antiferromagnets, given the almost isotropic g values. In such solids there are two possible low-temperature instabilities that arise from the weak transverse coupling between the spin chains, the spin-Peierls (1-D) and SDW antiferromagnetic (3-D) instabilities. Below the spin-Peierls transition the spin chain dimerizes gradually to form a nonmagnetic singlet state at 0 K; thus, the susceptibility along any direction is exponential up to the transition temperature. The antiferromagnetic instability leads to a 3-D ordered spin lattice, in which, as the temperature tends to zero, the susceptibility tends to zero along the preferred spin direction, and to a constant value perpendicular to this direction. These two transitions can be differentiated clearly in both static susceptibility and EPR measurements. The average susceptibility tends to zero for a spin-Peierls and to a constant value for a 3-D antiferromagnet. The line width of the EPR signal is approximately constant in the spin-Peierls but diverges at the transition to a 3-D antiferromagnetic state, *e.g.*, β'-(BEDT-TTF)$_2$AuCl$_2$[42] and (BEDT-TTF)Ag$_4$CN$_5$.[43] The fall in the susceptibility of (BEDT-TTF)$_2$GaCl$_4$ at ~50 K may indicate such phase transitions, but the lack of any divergence in line width and g-value of the EPR resonance eliminates the possibility of a 3-D ordered antiferromagnetic state and the absence of a knee in the susceptibility and the poor fit to a uniform one-dimensional antiferromagnet suggest it is not a spin-Peierls transition. High-field magnetization will be needed to resolve these ambiguities.

The Hubbard model still applies to (BEDT-TTF)$_2$GaCl$_4$; since the BEDT-TTF molecules are dimerized the band structure is built up from the bonding and antibonding orbitals of a pair of BEDT-TTF molecules. The Coulomb repulsion energy, U (between electrons in the same molecular orbital), is large in this salt (usually $U \sim 1-1.4$ eV) so that these levels are only singly occupied, and there is an upper Hubbard level separated by an energy U from the lower levels. The Hubbard model predicts that the magnetic exchange energy is given by $J = 2t^2/U_{\text{eff}}$, where U_{eff} is the energy to put two spins on the same site. Since the repulsion energy between two electrons occupying the same orbital is larger than the energy difference between the bonding and antibonding levels ($=2t_1$), the lowest energy state becomes the one with one electron occupying the bonding orbital and one the antibonding orbital. This requires an energy $2t_1$, so $U_{\text{eff}} = 2t_1$, an energy that is independent of the on-site interaction U. For a real system of dimers the interdimer transfer integral t_2 broadens the energy levels so that U_{eff} is reduced to $U_{\text{eff}} = 2(t_1 - t_2)$. The semiconducting energy gap is given by $E_g = U_{\text{eff}}/2 = (t_1 - t_2)$, since exciting an electron to the upper band, with energy U_{eff}, creates two charge carriers, an electron and a hole. For (BEDT-TTF)$_2$GaCl$_4$ the same considerations apply (although the charges on the BEDT-TTF molecules are holes and not electrons), so that the exchange interaction is given by $J = 2t_2^2/U_{\text{eff}} = t_2^2/E_g$. Using $J/k_B \sim 70$ K and $E_g = 0.4$ eV, the Hubbard model thus predicts a bandwidth $4t_2 \sim 0.3$ eV.

Conclusion

We have demonstrated that a good understanding of the electrical and magnetic properties of organic conductors with nonmagnetic anions is a prerequisite to the understanding of the interaction between moments from conduction electrons and those localized on anions. Magnetically, the organic cations in (BEDT-TTF)$_2$GaCl$_4$ and (BEDT-TTF)$_2$FeCl$_4$ behave as dimers, the former containing two dimers with different singlet−triplet energy separations and the latter with a single singlet−triplet gap. The difference between the two compounds can be traced to the crystal structures, since the unit cell in the former is double that of the latter. The observed susceptibility is the sum of contributions from the organic and inorganic moieties, and there is no measurable exchange between the two spin sublattices.

Acknowledgment. This work was supported by the EPSRC, British Council (Alliance Programme), and EU (Human Capital and Mobility Programme (Network on Molecular Superconductors)). This manuscript was written while on a visit, funded by a British Council−Monbusho collaborative program, to the Japan Advanced Institute of Science and Technology at Hokuriku, Japan. M.K. thanks Professors T. Mitani and Y. Iwasa and Dr. H. Kitagawa for many discussions. We thank Dr. D. Watkin (Oxford University) for his help with the crystallography and Prof. Z. Soos for useful discussions.

Supporting Information Available: Tables giving a summary of crystallographic and refinement data, anisotropic displacement parameters, and bond lengths and angles (9 pages). Ordering information is given on any current masthead page.

IC951456Y

(42) (a) Coulon, C.; Laversanne, R.; Amiell, J.; Delhaes, P. *J. Phys. Condens. Matter* **1986**, *19*, L753.

(43) Geiser, U.; Wang, H. H.; Gerdom, L. E.; Firestone, M. A.; Sowa, L. M.; Whangbo, M.-H.; Williams, J. M. *J. Am. Chem. Soc.* **1985**, *107*, 8305.